Comparison of Kalman Smoother to Wiener Smoother in Practical OFDM Channel Estimation

Junichiro Hagiwara*, Toshihiko Nishimura†, Takeo Ohgane†, and Yasutaka Ogawa†
*Radio Access Network Development Department, NTT DOCOMO, INC.
3-5 Hikari-no-oka, Yokosuka-shi, Kanagawa, 239-8536 Japan
Email: hagiwaraj@nttdocomo.com
†Graduate School of Information Science and Technology, Hokkaido University
Kita 14 Nishi 9, Kita-ku, Sapporo, Hokkaido, 060-0814 Japan
Email: {nishim, ohgane, ogawa}@ist.hokudai.ac.jp

***Abstract*—Regarding linear estimation theory, the equivalence of the Wiener and Kalman filters is a well-known topic; however, the difference in a practical environment has not been thoroughly discussed. This paper compares the Kalman smoother to the Wiener smoother in terms of practical orthogonal frequency division multiplexing channel estimation on the receiver side. First, conditions for fair comparison are discussed. Under these conditions, the performance and complexity for both methods are numerically investigated. Comparison results show that the Wiener smoother slightly outperforms the Kalman smoother because it avoids cumulative error in sequential processing, while the complexity of the Kalman smoother is always lower than that for the Wiener smoother because there is no large matrix operation.**

I. Introduction

In recent years, the use of wireless communication devices such as mobile phones has become widespread, leading to a desire for more wireless speed and capacity. Orthogonal frequency division multiplexing (OFDM) transmission is an attractive technology that meets these needs. OFDM transmission is reliable and suited to wideband technology even in multipath environments, and has already been implemented in 3rd Generation Partnership Project Long Term Evolution (3GPP LTE), wireless local area networks, and terrestrial digital broadcasting. In mobile communication, multipath fading is a fundamental and unavoidable issue. One approach to cope with it is to estimate and then compensate for the fading channel on the receiver side. Improving channel estimation accuracy is very important because doing so ultimately leads to improved radio capacity. Proposals regarding OFDM channel estimation [1] are roughly grouped into two methods: the batch method, which considers multiple received symbols together, and the sequential method, which considers each received symbol individually. In [2], one of the authors proposed a sequential OFDM channel estimation method based on the Kalman filter [3]. On the other hand, the batch OFDM channel estimation method is also applicable to the same problem when latency is tolerated. The Wiener filter[1] [4] is the most popular batch method. Literature such as [5] sometimes describes the Wiener filter as theoretically equivalent to the Kalman filter under some conditions. However, it is considered that there is no literature that discusses a detailed comparison in a practical environment. Therefore, this paper compares both methods in practical OFDM channel estimation and summarizes the resulting knowledge. Note that OFDM channel estimation in this paper means estimation of narrow-band channel gains[2] for pilot signals on the receiver side.

The rest of this paper is structured as follows. Section II describes the investigation assumptions and problem formulation. Section III describes the conditions for fair comparison. Section IV presents numerical analysis results for the comparison. Section V summarizes the discussion.

II. Investigation Assumptions and Problem Formulation

A. Investigation Assumptions

A small-scale fading channel for known pilot signals is sequentially estimated on the receiver side in an OFDM transmission environment. The frequency interval between OFDM subcarriers is designed to be sufficiently wide to ignore any inter-subcarrier interference caused by the Doppler effect. The pilot subcarrier is not coded and is scattered in a comb pattern [6] in the time and frequency domains. dt and df denote the time and frequency intervals between adjacent pilot subcarriers, respectively. Multipath wave characteristics are determined by wide-sense stationary uncorrelated scattering (WSSUS) [7] and are invariant over the OFDM symbol duration. The maximum multipath wave delay is shorter than the OFDM guard interval (GI). In order to model time and frequency selectivity, many independent measurements are needed; however, for simplicity, this paper assumes typical models for land mobile communications [8]. Time selectivity is based on the Jakes' model [9] and frequency selectivity is based on the exponential delay profile [9]. The fading channel obeys a stationary stochastic process. This implies that hyperparameters such as the Doppler frequency, delay spread, and E_b/N_0 are time-invariant during the study period. Furthermore, true hyperparameters are assumed to be known for simplicity. The nonlinearity of the employed analog radio circuit and imperfections in time, phase, and frequency at coherent detection are all negligible. This paper considers only a single-input, single-output environment.

The following description pertains to notational assumptions. $\mathbf{E}_k$ denotes the k-by-k identity matrix. For any matrix $\mathbf{A}$, $\mathbf{A}^{\mathrm{T}}$ denotes its transpose matrix, $\mathbf{A}^{\mathrm{H}}$ denotes its complex

[1]This is also called a linear minimum mean squared error (LMMSE) filter.

[2]This is also called the channel frequency response (CFR).

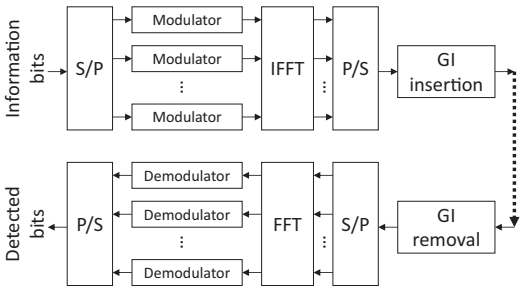

Fig. 1. Diagram of the OFDM transmitter and receiver in an equivalent baseband system.

conjugate transpose matrix, $\mathbf{A}^{-1}$ denotes its inverse matrix, and $\mathbf{A}^{1/2}$ denotes its square root matrix[3]. $\mathrm{diag}(A_0, A_1, \ldots)$ denotes a matrix in which each element in parentheses is sequentially set to the diagonal element. $\mathbf{A} = \{a(\mathrm{row}, \mathrm{col})\}$ denotes that the row-th and the column-th entry of $\mathbf{A}$ is defined by function a. $\otimes$ denotes the Kronecker product. $\mathbf{0}_k$ denotes the k-by-1 zero vector. When random vector $\mathbf{r}$ has an independent complex normal distribution with mean vector $\boldsymbol{\mu}$ and covariance matrix $\boldsymbol{\Gamma}$, the relationship is written as $\mathbf{r} \sim \mathcal{CN}(\boldsymbol{\mu}, \boldsymbol{\Gamma})$. For any value $\cdot$, $E[\cdot]$ denotes its time average, $|\cdot|$ denotes its absolute value, and $\hat{\cdot}$ denotes its estimator. j denotes imaginary unit $\sqrt{-1}$. $O(u)$ denotes that complexity is proportional to u.

B. Problem Formulation

This paper's approach for sequential OFDM channel estimation first estimates the narrow-band channel gains for pilot subcarriers and then interpolates that gains for non-pilot subcarriers. We discussed various interpolation methods [10] and found that appropriate methods already exist; thus, interpolation is beyond scope of this paper.

Fig. 1 shows the OFDM transmitter and receiver in an equivalent baseband system [11]. On the transmitter side, information bits are parallelized and modulated to the symbols of each subcarrier. An inverse fast Fourier transform is applied to these symbols, which are then serialized. A GI is appended to the output before the OFDM signal is transmitted. On the receiver side, the GI is removed from the received OFDM signal, the output is parallelized, and a fast Fourier transform is applied to the symbols of each subcarrier. These symbols are demodulated and serialized to detect information bits. The relationship between the received and transmitted pilot symbols is expressed as

$$\mathbf{y}^P(t) = \mathbf{S}^P(t)\tilde{\mathbf{h}}^P(t) + \mathbf{v}^P(t), \tag{1}$$

where superscript P for vector/matrix variables denotes that these consider pilot subcarriers only. $\mathbf{y}^P(t) = [y_0(t), \ldots, y_i(t), \ldots, y_{I-1}(t)]^{\mathrm{T}}$ denotes the I-by-1 received pilot symbol vector at the t-th symbol, and its subscript denotes a pilot subcarrier index in the frequency domain. I corresponds to the maximum number of pilot subcarriers in one symbol duration. $\mathbf{S}^P(t) = \mathrm{diag}(s_0(t), \ldots, s_i(t), \ldots, s_{I-1}(t))$ denotes the I-by-I transmitted pilot symbol matrix at the t-th symbol. $\tilde{\mathbf{h}}^P(t) = [\tilde{h}_0(t), \ldots, \tilde{h}_i(t), \ldots, \tilde{h}_{I-1}(t)]^{\mathrm{T}}$ denotes the narrow-band channel gain vector of pilot subcarriers at the t-th symbol. $\mathbf{v}^P(t) \sim \mathcal{CN}(\mathbf{0}_I, \mathbf{V}^P)$ denotes the I-by-1 additive white Gaussian noise vector at the t-th symbol, and when σ^2 is assumed to be the average noise power of each subcarrier, $\mathbf{V}^P$ can be expressed as $\mathbf{V}^P = \sigma^2\mathbf{E}_I$.

[3]This matrix satisfies the relationship $\mathbf{A} = \mathbf{A}^{1/2}(\mathbf{A}^{1/2})^{\mathrm{H}}$.

For the OFDM channel estimation, various formulations of the Kalman and Wiener filters have been proposed [1], [2], [6], [10], [12]. This paper supposes the following formulations that are considered to be the most basic.

1) Kalman Filter: The formulation of the Kalman filter is based on the state-space model according to [2], but the extended formulation for complexity reduction is not considered. Observation and state equations for the state-space model are expressed as

$$\mathbf{y}^P(t) = \mathbf{F}^P(t)\,\boldsymbol{\theta}^P(t) + \mathbf{v}^P(t), \tag{2}$$
$$\boldsymbol{\theta}^P(t) = \mathbf{G}^P(t)\,\boldsymbol{\theta}^P(t-1) + \mathbf{w}^P(t), \tag{3}$$

where $\mathbf{y}^P(t)$ denotes the I-by-1 observation vector for pilot subcarriers at the t-th symbol (as in (1)), $\mathbf{F}^P(t)$ denotes the I-by-I observation matrix for pilot subcarriers at the t-th symbol, $\boldsymbol{\theta}^P(t) = [\theta_0(t), \ldots, \theta_i(t), \ldots, \theta_{I-1}(t)]^{\mathrm{T}}$ denotes the I-by-1 state vector for pilot subcarriers at the t-th symbol, and $\mathbf{G}^P(t)$ denotes the I-by-I transition matrix for pilot subcarriers at the t-th symbol. $\mathbf{v}^P(t) \sim \mathcal{CN}(\mathbf{0}_I, \mathbf{V}^P)$ denotes the I-by-1 observation noise vector for pilot subcarriers at the t-th symbol; its covariance matrix is set to $\mathbf{V}^P = \mathrm{diag}(V_0, \ldots, V_i, \ldots, V_{I-1})$ (as in (1)). $\mathbf{w}^P(t) \sim \mathcal{CN}(\mathbf{0}_I, \mathbf{W}^P)$ denotes the I-by-1 state noise vector for pilot subcarriers at the t-th symbol; its covariance matrix is set to $\mathbf{W}^P = \mathrm{diag}(W_0, \ldots, W_i, \ldots, W_{I-1})$.

Detailed definitions regarding the observation equation are given below:

$$\tilde{\mathbf{h}}^P(t) = \boldsymbol{\Sigma}^P\,\boldsymbol{\theta}^P(t), \tag{4}$$
$$\mathbf{F}^P(t) = \mathbf{S}^P(t)\boldsymbol{\Sigma}^P, \tag{5}$$
$$\boldsymbol{\Sigma}^P = \left(\boldsymbol{\Omega}_f^P\right)^{1/2}, \tag{6}$$
$$\boldsymbol{\Omega}_f^P = \{\rho\,(\Delta t = 0,\, \Delta f = (\mathrm{col} - \mathrm{row})df)\,\}, \tag{7}$$
$$\rho(\Delta t = 0, \Delta f) = \frac{1 + j2\pi\Delta f\sigma_\tau}{1 + (2\pi\Delta f\sigma_\tau)^2}, \tag{8}$$

where $\rho(\Delta t, \Delta f)$ denotes the time and frequency correlation coefficient of the narrow-band channel gain, Δt denotes the time difference, Δf denotes the frequency difference, and σ_τ denotes the channel delay spread.

Detailed definitions regarding the state equation are given below:

$$\mathbf{G}^P(t) = \mathbf{E}_I, \tag{9}$$
$$\mathbf{W}^P = 2m^2(1 - \rho(\Delta t = 1dt, \Delta f = 0))\mathbf{E}_I, \tag{10}$$
$$\rho(\Delta t, \Delta f = 0) = J_0(2\pi f_D \Delta t), \tag{11}$$

where m^2 denotes the average power of the narrow-band channel gain for each pilot subcarrier, J_0 represents Bessel functions of the first kind of order zero [9], and f_D denotes the channel maximum Doppler frequency.

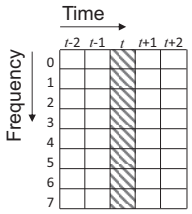

Fig. 2. Estimated pilot signals for smoothing ($L = 2$ and $I = 8$).

2) Wiener Filter: The formulation of the Wiener filter is based on [12, eq. (41)]:

$$\hat{\mathbf{H}}^P = \mathbf{\Omega}_{tf}^P \left(\mathbf{\Omega}_{tf}^P + \frac{\beta}{\mathrm{SNR}} \mathbf{E}_I \right)^{-1} \hat{\mathbf{H}}_{\mathrm{LS}}^P, \tag{12}$$

$$\hat{\mathbf{H}}^P = \left[\hat{\mathbf{h}}^P(t-L)^{\mathrm{T}}, \ldots, \hat{\mathbf{h}}^P(t)^{\mathrm{T}}, \ldots, \hat{\mathbf{h}}^P(t+L)^{\mathrm{T}} \right]^{\mathrm{T}}, \tag{13}$$

$$\mathbf{\Omega}_{tf}^P = \begin{cases} \mathbf{\Omega}_t^P \otimes \mathbf{\Omega}_f^P & \text{for upper diagonal elements} \\ & \text{of } \mathbf{\Omega}_t^P, \\ \mathbf{\Omega}_t^P \otimes (\mathbf{\Omega}_f^P)^{\mathrm{H}} & \text{otherwise,} \end{cases} \tag{14}$$

$$\mathbf{\Omega}_t^P = \{ \rho \, (\Delta t = |\mathrm{col} - \mathrm{row}| dt, \, \Delta f = 0) \}, \tag{15}$$

$$\beta = E[|s_i(t)|^2] \, E[1/|s_i(t)|^2], \tag{16}$$

$$\hat{\mathbf{H}}_{\mathrm{LS}}^P = \left[\hat{\mathbf{h}}_{\mathrm{LS}}^P(t-L)^{\mathrm{T}}, \ldots, \hat{\mathbf{h}}_{\mathrm{LS}}^P(t)^{\mathrm{T}}, \ldots, \hat{\mathbf{h}}_{\mathrm{LS}}^P(t+L)^{\mathrm{T}} \right]^{\mathrm{T}}, \tag{17}$$

$$\hat{\mathbf{h}}_{\mathrm{LS}}^P(t) = \mathbf{S}^P(t)^{-1} \mathbf{y}^P(t), \tag{18}$$

where the batch time period corresponds to $2L + 1$ symbols.

III. Conditions for Fair Comparison

A. Type of Estimation

When the data at the t-th symbol are estimated using the data up to the k-th symbol, the estimation is generally classified into the following three types depending on the relationship between t and k:

$$\begin{cases} \text{Filtering} & \text{if } t = k, \\ \text{Prediction} & \text{if } t > k, \\ \text{Smoothing} & \text{if } t < k. \end{cases}$$

This paper supposes *smoothing* for the ease of comparison. Regarding the Wiener filter, $\hat{\hat{\mathbf{h}}}^P(t)$ in Section II-B2 straightforwardly corresponds to a smoothing estimator. For example, when $L = 2$ and $I = 8$, estimated pilot signals for smoothing are represented by the hatched area in Fig. 2. The batch smoothing process in this paper is hereafter referred to as the Wiener smoother. On the other hand, adapted to the Wiener smoother, the Kalman filter requires a backward smoothing process in addition to that in Section II-B1. When the popular Rauch-Tung-Striebel (RTS) algorithm [13] is applied to the backward smoothing process, backward recursion in this study is expressed as

$$\begin{aligned} &\text{Smoothing estimator (mean) of state: } \hat{\boldsymbol{\theta}}_{\mathrm{S}}^P(t) \\ &= \hat{\boldsymbol{\theta}}^P(t) + \mathbf{C}^P(t) \mathbf{G}^P(t+1)^{\mathrm{H}} \mathbf{R}^P(t+1)^{-1} \left(\hat{\boldsymbol{\theta}}_{\mathrm{S}}^P(t+1) - \mathbf{a}^P(t+1) \right) \\ &= \hat{\boldsymbol{\theta}}^P(t) + \mathbf{C}^P(t) \mathbf{R}^P(t+1)^{-1} \left(\hat{\boldsymbol{\theta}}_{\mathrm{S}}^P(t+1) - \mathbf{a}^P(t+1) \right), \end{aligned} \tag{19}$$

where definitions of $\hat{\boldsymbol{\theta}}^P(t)$, $\mathbf{C}^P(t)$, $\mathbf{a}^P(t)$, and $\mathbf{R}^P(t)$ are according to [2]; $\hat{\boldsymbol{\theta}}^P(t)$ and $\mathbf{C}^P(t)$ denote filtered estimators (mean and variance, respectively) of state; and $\mathbf{a}^P(t)$ and $\mathbf{R}^P(t)$ denote one-step-ahead prediction (mean and variance, respectively) of state. The RTS algorithm implicitly assumes that the Kalman filter has been swept in advance, so $\hat{\boldsymbol{\theta}}^P(t)$, $\mathbf{C}^P(t)$, $\mathbf{a}^P(t)$, and $\mathbf{R}^P(t)$ are assumed to be already calculated and stored via the advanced Kalman filter. The sequential smoothing process in this paper is hereafter referred to as the Kalman smoother.

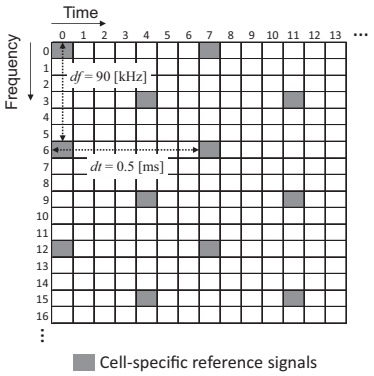

Fig. 3. Scattered pilot subcarrier allocation.

TABLE I
Computer simulation assumptions

Carrier frequency	2 [GHz]
Maximum Doppler frequency: f_D	14 [Hz] (i.e., 7.6 [km/h])
Delay profile	• 24-path exponential – Delay spread: 1 [μs] – Maximum delay: 4.7 [μs] (within GI)
Numerical computation of Kalman filter/smoother	A square root Kalman filter/smoother based on singular value decomposition [15] is applied to suppress the degradation in numerical accuracy.

B. Fixed Time Lag L

The fixed time lag, L, in both the Kalman and Wiener smoothers must be specified in a practical smoothing process. Lag L should be the required minimum because sequential processing may yield cumulative error unlike batch processing. To determine this value, a computer simulation is performed using 3GPP LTE specifications with a 5 MHz bandwidth. The frequency interval between each subcarrier is 15 [kHz], and the symbol length (except for the GI) corresponds to 66.7 [μs]. Cell-specific reference signals (CRSs) [14] are regarded as pilot subcarriers. Fig. 3 shows the CRS allocation. In the figure, CRSs at timeslots 4, 11, $\cdots$ are not used in the simulation, dt = 0.5 [ms], df = 90 [kHz], and a specific pseudorandom sequence for the CRSs is modulated by QPSK. Thus, $\beta/\mathrm{SNR} = 1/(2E_b/N_0)$ in (12). There is a total of 300 subcarriers, and the number of pilot subcarriers for one symbol duration is 50. An isolated cell and single-user environment without inter-cell interference and multiple access are assumed. Table I shows the other assumptions used for the computer simulation.

Fig 4 shows the impact of L on the cumulative error in the Kalman smoother. In the figure, L (one slot corresponds to one dt) is denoted on the X-axis and the normalized mean squared error (NMSE) = $\sum_{i=0}^{I-1} E[|\tilde{h}_i(t) - \hat{\tilde{h}}_i(t)|^2] \,/\, \sum_{i=0}^{I-1} E[|\tilde{h}_i(t)|^2]$

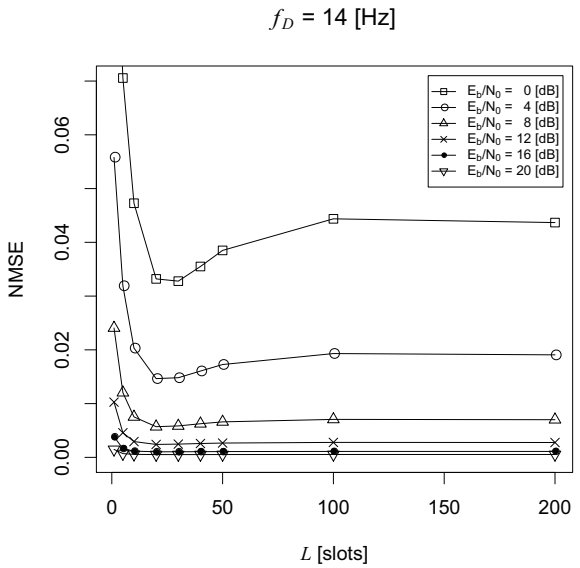

Fig. 4. Impact of L on the cumulative error in Kalman smoother.

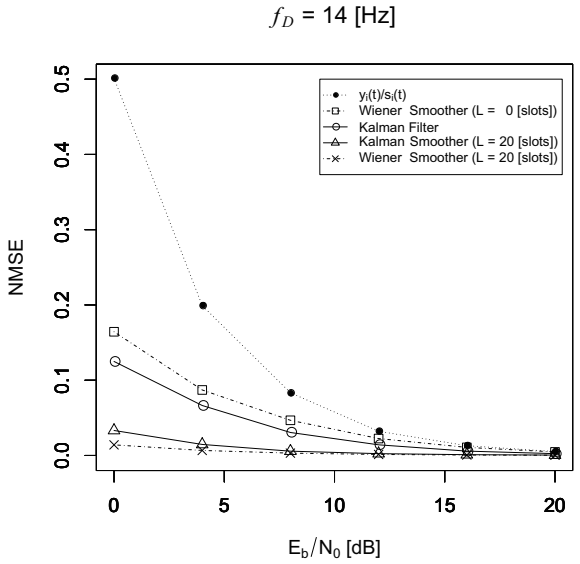

Fig. 5. NMSE performance.

is denoted on the Y-axis. The figure shows that L becomes optimal at around 20, so L is set to 20 [slots] (i.e., 10 [ms]) in the following investigation. This optimal L value corresponds to the time lag where the time correlation coefficient decreases from 1 to approximately 0.8 for f_D = 14 [Hz].

IV. Numerical Analysis

A. Performance Comparison

To compare the performance of NMSE and the bit error rate (BER), a computer simulation is performed under the same conditions as in Section III-B.

1) NMSE Performance: Fig. 5 shows the NMSE performance for f_D = 14 [Hz]. In the figure, E_b/N_0 is denoted on the X-axis and the NMSE is denoted on the Y-axis. Both the Kalman and Wiener smoothers at L = 20 exhibit good performance at almost the same level. However, the Wiener smoother at L = 20 slightly outperforms the Kalman smoother at L = 20. For example, at E_b/N_0 = 0 [dB], the Wiener smoother at L = 20 improves the NMSE by 0.02 compared to the Kalman smoother at L = 20. Cumulative error in the sequential processing yields this difference. The higher E_b/N_0 becomes, the smaller this cumulative error becomes. Thus, at E_b/N_0 = 20 [dB], the NMSE difference decreases to the negligible value of 0.0003.

TABLE II
Data subcarrier assumptions

Modulation	QPSK
Interpolation of channel estimator	• Frequency domain: Linear insertion • Time domain: The nearest neighbor
Equalization	• Zero forcing (ZF) [11] for LS channel estimator $y_i(t)/s_i(t)$ • Minimum Mean Squared Error (MMSE) [11] for the other channel estimators
Channel coding	• Convolutional codes – Rate: 1/2 – Constraint length: 7
Channel decoding	Soft-decision Viterbi algorithm
Interleaving	• Random interleaver – Unit: Symbol-by-symbol – Depth: 5 Resource blocks (RBs) [14], which corresponds to 400 symbols

The other performance levels such as the least-squares (LS) estimator, $y_i(t)/s_i(t)$, Wiener smoother at L = 0, and the Kalman filter are also plotted in Fig. 5 for deeper understanding. The LS estimator and Wiener smoother at L = 0 estimate a fading channel using not past and future information but current information only. The Wiener smoother at L = 0 further considers *frequency correlation* and outperforms the LS estimator. The Kalman filter estimates the fading channel using *past* and current information considering frequency correlation. Thus, the Kalman filter outperforms the Wiener smoother at L = 0. The Kalman and Wiener smoothers at L = 20 estimate the fading channel using all the past, current, and relative *future* information considering frequency correlation. Thus, the Kalman and Wiener smoothers at L = 20 outperform the Kalman filter. As a result, the more information that is used for the estimation, the higher the level of performance that can be archived essentially.

2) BER Performance: Fig. 6 shows the BER performance for f_D = 14 [Hz] using the data subcarrier assumptions given in Table II. The BER and E_b/N_0 are denoted on the Y-axis and X-axis, respectively. The BER performance improves in the same order as the NMSE performance in Fig. 5. Both the Kalman and Wiener smoothers at L = 20 exhibit almost the same performance close to Lower Bound 1. However, the Wiener smoother at L = 20 slightly outperforms the Kalman smoother at L = 20 due to the avoidance of cumulative error in the sequential processing. For example, at the BER of 10^{-4}, the Wiener smoother at L = 20 improves the coding gain by 0.8 dB compared to the Kalman smoother at L = 20.

B. Complexity Comparison

Complexity in this paper refers to the number of multiplications and divisions occurring during the smoothing process

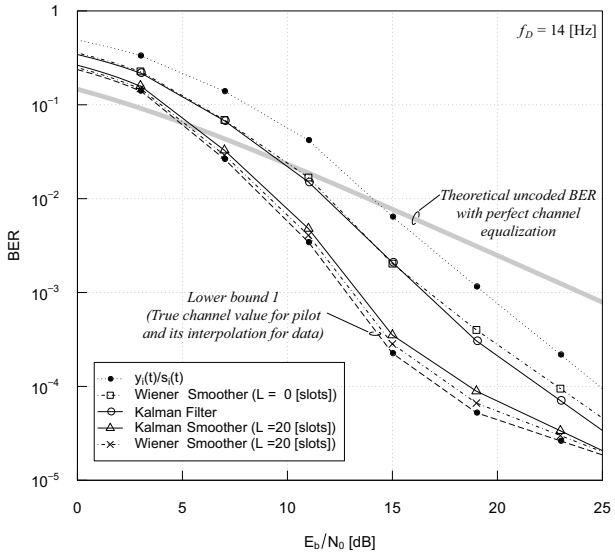

Fig. 6. BER performance.

TABLE III
COMPLEXITY FOR MATRICES PREPARED BEFORE SMOOTHING PROCESS

	Complexity	Note
$\mathbf{F}^P(t)$	$(2L+1)I^2 + I^3/6$	Refer to (5) and (6)
$\mathbf{\Omega}^P_{tf}$	$(2L+1)I$	Refer to Toeplitz and Hermitian (14)

TABLE IV
COMPLEXITY FOR SMOOTHING PROCESS

	Complexity	Note
Kalman filter	$5I^3 + 2I^2$ (for 1 step)	Refer to Table 1 in [2]
RTS algorithm	$I^3 + I^3 + I^2$ (for 1 step)	Refer to (19)
Derivation of $\tilde{\mathbf{h}}^P(t)$ from state	I^2 (for the t-th symbol)	Refer to (4)
Wiener smoother	$2((2L+1)I)^3 + ((2L+1)I)^2 + (2L+1)I$	Refer to (12)

which estimates the pilot signals at the t-th symbol. We assume pure matrix operations, and that the complexities of the inverse matrix derivation and Cholesky factorization are I^3 and $I^3/6$, respectively. In addition, we assume that the time and frequency correlation coefficients have been calculated in advance. Table III gives the complexity for the matrices prepared before the smoothing process. Note that $O(1)$ complexity such as the setting of $\mathbf{V}^P$ and $\mathbf{W}^P$ is omitted from Table III because it has negligible impact. Table IV also gives the complexity for the smoothing process itself. According to Tables III and IV, the complexity for the Kalman smoother is [Preparation of $\mathbf{F}^P(t)$] + $(2L+1)$[Kalman filter for 1 step] + L[RTS algorithm for 1 step] + [Derivation of $\tilde{\mathbf{h}}^P(t)$ from state for the t-th symbol] = $(12L + 5 + 1/6)I^3 + (7L + 4)I^2$, and that for the Wiener smoother is [Preparation of $\mathbf{\Omega}^P_{tf}$] + [Wiener smoother] = $2(2L+1)^3I^3+(2L+1)^2I^2+2(2L+1)I$. Thus, the complexity for the Kalman smoother is always lower than that for the Wiener smoother for any integer $L \geq 0$ and $I \geq 1$. The major reason for this result depends on the presence or absence of a large matrix operation. In particular, the coefficient of I^3 for the Wiener smoother reaches $O(L^3)$, while that for the Kalman smoother remains at $O(L)$. According to this fact, the longer L becomes, the higher the complexity ratio of the Wiener smoother to the Kalman smoother becomes. For example, the ratio reaches 556 for $L = 20$ and $I = 50$.

V. CONCLUSIONS

This paper compared the Kalman smoother to the Wiener smoother in terms of practical OFDM channel estimation on the receiver side. These two methods are theoretically equivalent but practically different. First, the conditions for fair comparison were discussed. Regarding the smoothing process, the fixed time lag should be set to the required minimum, because sequential processing yields cumulative error. The optimal value corresponds to the time lag where the time correlation coefficient decreases from 1 to approximately 0.8 for $f_D = 14$ [Hz]. The results of numerical analysis lead to the following conclusions.

- Performance (NMSE and BER): Both the Kalman and Wiener smoothers exhibit almost the same good performance levels. However, the Wiener smoother slightly outperforms the Kalman smoother because it avoids cumulative error in the sequential processing. The NMSE and coding gain improvements using the Wiener smoother reach, at most, 0.02 and 0.8 dB, respectively, compared to those for the Kalman smoother.
- Complexity: Regarding the number of multiplications and divisions occurring during the smoothing process which estimates the pilot signals at some symbols, the complexity of the Kalman smoother is always lower than that for the Wiener smoother because there is no large matrix operation. For example, the complexity ratio of the Wiener smoother to the Kalman smoother reaches 556 for $L = 20$ and $I = 50$.

According to the above, we recognize that the Kalman and Wiener smoothers have different advantages; the Kalman filter has a lower complexity level whereas the Wiener filter yields better performance.

REFERENCES

[1] L. Hanzo, M. Münster, B. Choi, and T. Keller, *OFDM and MC-CDMA for broadband multi-user communications, WLANs and broadcasting*. John Wiley & Sons, 2003.

[2] J. Hagiwara, "An OFDM channel estimation method based on a state-space model that appropriately considers frequency correlation," *IEICE TRANSACTIONS on Fundamentals of Electronics, Communications and Computer Sciences*, vol. 98, no. 2, pp. 537–548, 2015.

[3] R. E. Kalman, "A new approach to linear filtering and prediction problems," *Journal of Basic Engineering, Transactions of the ASME*, vol. 82 (Series D), no. 1, pp. 35–45, 1960.

[4] N. Wiener, *Extrapolation, Interpolation, and Smoothing of Stationary Time Series*. Technology Press and Wiley, NY, 1949.

[5] T. Kailath, A. H. Sayed, and B. Hassibi, *Linear Estimation*. Prentice Hall Upper Saddle River, NJ, 2000.

[6] O. Simeone, Y. Bar-Ness, and U. Spagnolini, "Pilot-based channel estimation for OFDM systems by tracking the delay-subspace," *IEEE Transactions on Wireless Communications*, vol. 3, no. 1, pp. 315–325, 2004.

[7] P. Bello, "Characterization of randomly time-variant linear channels," *IEEE transactions on Communications Systems*, vol. 11, no. 4, pp. 360–393, 1963.

[8] Y. Karasawa, *Radiowave Propagation Fundamentals for Digital Mobile Communications*. Corona Publishing, 2003, (In Japanese).

[9] W. C. Jakes, Jr., *Microwave Mobile communications*. Wiley, New York, 1974, [reprinted by IEEE Press].

[10] D. Larsson, "Analysis of channel estimation methods for OFDMA," Master's thesis, Royal Institute of Technology (KTH), Stockholm, Sweden, 2006.

[11] A. Goldsmith, *Wireless communications*. Cambridge University Press, 2005.

[12] M. K. Ozdemir and H. Arslan, "Channel estimation for wireless OFDM systems," *IEEE Communications Surveys & Tutorials*, vol. 9, no. 2, pp. 18–48, 2007.

[13] H. E. Rauch, F. Tung, and C. T. Striebel, "Maximum likelihood estimates of linear dynamic systems," *AIAA journal*, vol. 3, no. 8, pp. 1445–1450, 1965.

[14] *Evolved Universal Terrestrial Radio Access (E-UTRA); Physical channels and modulation*, The 3rd Generation Partnership Project (3GPP) TS 36.211, Dec. 2009.

[15] L. Wang, G. Libert, and P. Manneback, "Kalman filter algorithm based on singular value decomposition," in *Proceedings of the 31st IEEE Conference on Decision and Control*, 1992, pp. 1224–1229.